The highly excited C–H stretching states of CHD_3, CHT_3, and CH_3D

Gregory A. Voth, R. A. Marcus, and A. H. Zewail[a)]
Arthur Amos Noyes Laboratory of Chemical Physics,[b)] California Institute of Technology, Pasadena, California 91125

(Received 9 July 1984; accepted 11 September 1984)

Unlike many other molecules having local modes, the highly excited C–H stretching states of CHD_3 show well resolved experimental spectra and simple Fermi resonance behavior. In this paper the local mode features in this prototype molecule are examined using a curvilinear coordinate approach. Theory and experiment are used to identify the vibrational state coupling. Both kinetic and potential terms are employed in order to characterize the coupling of the C–H stretch to various other vibrational modes, notably those including D–C–H bending. Predictions are also made for CHT_3 and the role of dynamical coupling on the vibrational states of CH_3D explored. Implications of these findings for mode-specific and other couplings are discussed.

I. INTRODUCTION

The highly excited vibrational states of C–H stretching modes in many molecules have been the subject of considerable interest in recent years.[1] The local mode description[1] has been used to treat these C–H oscillator systems and has had considerable success in doing so. Of particular relevance to the present paper are the experimental results of Perry *et al.*[2] which, for CHD_3, indicate the specific coupling of the C–H stretch to a bending normal mode. For other molecules, this type of coupling has been discussed previously by several authors.[3] The local mode description has recently been extended to handle such couplings,[4] using curvilinear coordinate systems.[5–7] These coordinate systems present a natural way of treating molecular vibrations and provide physical insight into the coupling mechanisms between vibrational states. To such vibrational couplings have been attributed the calculated breakdown of localized C–H stretching vibrations,[1–4,8,9] the observed linewidths of aromatic ($\sim$100–200 cm^{-1}) and aliphatic ($\sim$20 cm^{-1}) local mode transitions,[4,9–11] and the postulated onset of extensive intramolecular relaxation.[4,9,12,13]

With these aspects in mind, the highly excited C–H stretching vibrations in CHD_3, CHT_3, and CH_3D are studied in the present paper. Recent experimental evidence[2] has suggested that in CHD_3 there are extremely narrow linewidths (< 1 cm^{-1}) and very limited state mixing at a high level of C–H vibrational excitation. An analysis of this spectral data was performed in terms of a simple Fermi resonance between the C–H stretch and a bending normal mode.[2] In the present paper, using a curvilinear coordinate treatment, a theoretical analysis is presented for the vibrational eigenstate problem which includes kinetic and potential energy coupling terms. An explanation for the observed spectrum of CHD_3 is proposed and, in turn, predictions are made for the high overtone C–H stretching spectrum of CHT_3. In addition, the difference between the relatively simple CHD_3 spectrum and the highly congested spectrum[2] for CH_3D is discussed in terms of the different dynamical vibrational mode couplings in these two molecular species.

An outline of the present paper is as follows: A brief review of the relevant experimental data[2] is given in Sec. II. In Sec. III, the curvilinear coordinate formalism is applied to CHD_3 and CHT_3, and couplings between the C–H stretching vibration and other normal modes of these molecules are described. In Sec. IV, the dynamical coupling of the C–H stretching states to bending normal modes in CH_3D is examined. Concluding remarks appear in Sec. V.

II. CHD_3 AND CH_3D: SUMMARY OF THE EXPERIMENTAL RESULTS

Recently, using photoacoustic spectroscopy, the high C–H overtones of methane and of its isotopic derivatives CH_3D, CH_2D_2, and CHD_3 have been studied by Perry *et al.*[2] Some results obtained for CHD_3 and CH_3D, both of which have very different spectra, can be summarized as follows:

The CHD_3 overtones corresponding in zeroth order to five, six, and seven quanta in the C–H stretch have remarkable simplicity.[2] For $v = 5$ and $v = 6$, the spectra have a simple two level Fermi resonance structure (e.g., Fig. 1 for $v = 6$). For $v = 7$, the spectrum is more congested, but it appears to be essentially a three level Fermi resonance.[2] When the quantity $\Delta E_{ov}/v$ is plotted vs v, ΔE_{ov} being the excitation of the C–H overtone in excess of the zero-point

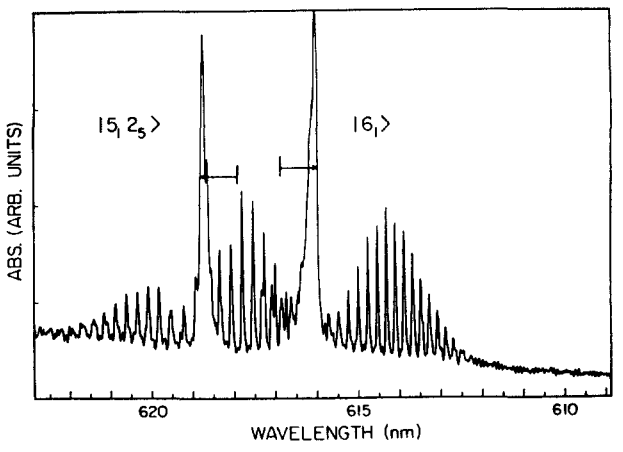

FIG. 1. Experimental $v = 6$ C–H overtone spectrum for CHD_3 (taken from Ref. 2).

[a)] Camille and Henry Dreyfus Teacher–Scholar.
[b)] Contribution no. 7057.

 0021-9606/84/245494-14$02.10

energy, one obtains[2] an excellent Birge–Sponer line,[1] but with deviations in the $v = 5$, 6, and 7 regions where these Fermi resonances become important. Also, the CHD_3 spectra clearly show the P-, Q-, and R-like branches expected for a symmetric top molecule with parallel type vibrational/rotational transitions.[14] Considering the size of the molecule involved and the density of vibrational states, the simplicity of these spectra is quite interesting.

The spectrum at $v = 6$ for CH_3D (Fig. 2), on the other hand, is strikingly different from that for CHD_3 at the same level of excitation. This transition has a spectral envelope with a width at half-maximum of approximately 150 cm^{-1}. The excitation of the C–H stretching states in this molecule corresponds to both parallel and perpendicular type vibrational/rotational transitions[14] and therefore has more complicated selection rules than that for CHD_3. The level structure underneath the spectral envelope at $v = 6$ is expected to be quite complicated for this and other reasons.

Several compelling questions arise from the experimental data on these two molecules. For instance, why do the $v = 5$ and $v = 6$ transitions in CHD_3 have such a remarkably simple level structure? A harmonic state count[15] yields a density of A_1 symmetry vibrational states of about 35 states/cm^{-1} at the energy of the $v = 6$ transition. There are, thereby, many vibrational states with the proper symmetry to couple with the C–H stretch (which has A_1 symmetry) via Fermi resonance interactions. The behavior actually observed is highly nonstatistical, however, since very few states are significantly coupled. In addition, the observed CHD_3 spectrum at $v = 6$ is very different from the corresponding CH_3D spectrum, and a knowledge of the mechanism that causes the high degree of congestion in the latter is of particular interest.

III. THEORY FOR CHD_3, CHT_3

A. Curvilinear formalism: qualitative analysis for CHD_3

The general expression for the classical vibrational Hamiltonian in curvilinear interval valence displacement coordinates[5,7] is

$$H(\mathbf{x},\mathbf{p}) = \frac{1}{2}\sum_{ij}^{N} G_{ij}(\mathbf{x}) p_i p_j + V(\mathbf{x}), \tag{3.1}$$

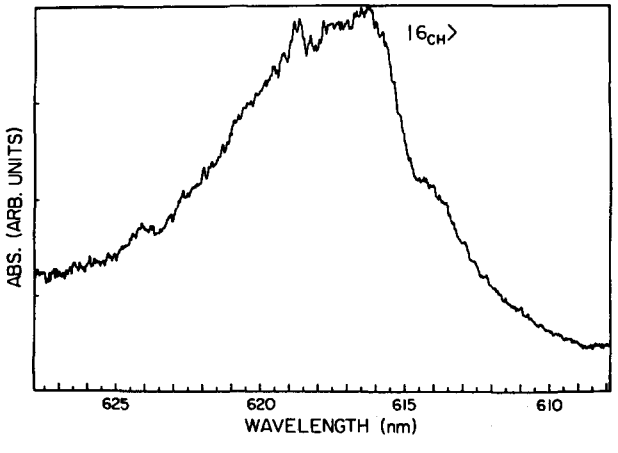

FIG. 2. Experimental $v = 6$ C–H overtone spectrum for CH_3D (taken from Ref. 2).

where the $G_{ij}(\mathbf{x})$ are the Wilson G-matrix elements[16] which, in the curvilinear coordinate approach, are dynamical functions of the curvilinear displacement coordinates $\mathbf{x}$, and $V(\mathbf{x})$ is some Born–Oppenheimer potential energy surface for the molecular vibrations. In the rectilinear coordinate approach,[6,7,16] the G-matrix elements are treated as constants and the potential $V(\mathbf{x})$ contains extra contributions to compensate for this restriction.

For any particular molecular vibrational problem, one must usually make some approximation for the potential energy function $V(\mathbf{x})$, since this quantity is rarely known accurately. For the analysis of the vibrations in CHD_3, it will first be assumed that the single C–H stretching mode may be described by a Morse oscillator potential energy function[17] and that the remaining vibrations are adequately described by harmonic (quadratic) potentials. The coupling between modes is then qualitatively described by the dynamical dependence of the G-matrix terms in Eq. (3.1). It will be shown later in this paper that, in addition to these G-matrix couplings, higher order (i.e., higher than quadratic) curvilinear potential energy terms are needed in order to explain more quantitatively the observed spectra of CHD_3.

The corresponding quantum mechanical Hamiltonian to Eq. (3.1) may be defined in effect by substituting the momentum operator $\hat{p}_i = (\hbar/i)\partial/\partial x_i$ for p_i in Eq. (3.1). This step is not rigorously exact, but it is an excellent approximation for the limit of relatively small amplitude molecular vibrations. A discussion of this appears in Ref. 7.

The Hamiltonian [Eq. (3.1)] for CHD_3 may be straightforwardly transformed into

$$H = H_0 + V', \tag{3.2}$$

where

$$H_0 = H_m(r,p) + \frac{1}{2}\sum_{i=2}^{9}(P_i^2 + \omega_i^2 Q_i^2) \tag{3.3a}$$

and the perturbation V' is given by

$$V' = \frac{1}{2}\sum_{i=2}^{9}[\tilde{G}_{ii}(\mathbf{x}) - 1]P_i^2 + \frac{1}{2}\sum_{i=2}^{9}\sum_{j=2}^{9}\tilde{G}_{ij}(\mathbf{x})P_iP_j. \tag{3.3b}$$

In these equations, $H_m(r,p)$ is the Morse oscillator Hamiltonian[17,18] for the C–H stretch with displacement coordinate r and conjugate momentum p; the $\frac{1}{2}(P_i^2 + \omega_i^2 Q_i^2)$ are the harmonic oscillator Hamiltonians for the eight curvilinear normal mode vibrations in CHD_3. Also, the $\tilde{G}_{ij}$'s are the G-matrix terms transformed via a normal mode transformation[16]

$$\tilde{G}_{ij}(\mathbf{x}) = \sum_{l=1}^{9}\sum_{m=1}^{9} L_{il}^{-1}\bar{G}_{lm}(\mathbf{x})L_{jm}^{-1}, \tag{3.4}$$

where the $\bar{G}_{lm}$'s are the G-matrix terms transformed via a symmetry coordinate transformation[16]

$$\bar{G}_{lm}(\mathbf{x}) = \sum_{i=1}^{9}\sum_{j=1}^{9} U_{li}G_{ij}(\mathbf{x})U_{mj}. \tag{3.5}$$

The coefficients U_{li} and L_{il}^{-1}, etc. in these equations are the elements of the matrices $\mathbf{U}$ and $\mathbf{L}^{-1}$ that define the transformations

$$\mathbf{q} = \mathbf{U}\mathbf{x}, \quad \mathbf{Q} = \mathbf{L}^{-1}\mathbf{q} \tag{3.6}$$

TABLE I. Internal symmetry coordinates for $CHD_3(CHT_3)$.[a]

$$q_1^{A_1} = r$$
$$q_2^{A_1} = \frac{1}{\sqrt{3}}(r_1 + r_2 + r_3)$$
$$q_3^{A_1} = \frac{1}{\sqrt{6}}(\alpha_1 + \alpha_2 + \alpha_3 - \beta_1 - \beta_2 - \beta_3)$$
$$q_4^{E_a} = \frac{1}{\sqrt{6}}(2r_1 - r_2 - r_3)$$
$$q_5^{E_a} = \frac{1}{\sqrt{6}}(2\alpha_1 - \alpha_2 - \alpha_3)$$
$$q_6^{E_a} = \frac{1}{\sqrt{6}}(2\beta_1 - \beta_2 - \beta_3)$$
$$q_7^{E_b} = \frac{1}{\sqrt{2}}(r_2 - r_3)$$
$$q_8^{E_b} = \frac{1}{\sqrt{2}}(\alpha_2 - \alpha_3)$$
$$q_9^{E_b} = \frac{1}{\sqrt{2}}(\beta_2 - \beta_3)$$

[a] r is defined here to be the C–H bond displacement coordinate, r_i the C–D(T) bond displacement coordinates, α_i the D–C–D(T–C–T) angles opposite r_i, and β_i the H–C–D(T) angles that include the r_i bond.

to curvilinear symmetry coordinates $\mathbf{q}$ and normal coordinates $\mathbf{Q}$, respectively. The symmetry coordinates for CHD_3 are given in Table I while the $\mathbf{L}^{-1}$ matrix is the standard normal mode matrix calculated by the methods of Ref. 16 with all internal coordinates in the G-matrix terms evaluated at their equilibrium value. In order that the C–H coordinate r be treated as a local mode coordinate, the transformation coefficient L_{11}^{-1}, where coordinate 1 is defined as r, is set equal to unity and the coefficients L_{1i}^{-1}, L_{i1}^{-1} are set equal to zero for $i \neq 1$. This approximation does not diagonalize all the off-diagonal quadratic perturbation terms, leaving terms proportional to rQ_i and pP_i. However, the present calculations show these to be very small and they may be safely neglected. This approximation has been known since the early days of normal mode theory[8] and is a good one due to the high frequency of the C–H stretching vibrations; they are essentially adiabatic from the rest of the normal modes of a molecule when coupling terms of quadratic order only are treated. Thus, to quadratic order, the C–H stretching vibrations may be treated separately rather than included in the zeroth order normal mode analysis.

A principal approximation of this paper is to treat the dynamical G-matrix elements in Eqs. (3.1) and (3.3b) as functions of the C–H displacement coordinate r only. This approximation is assumed to be valid because, for the states of experimental interest in CHD_3,[2] the C–H stretching local mode is the only vibrational mode with appreciable amplitude. The other internal coordinates of the molecule are taken to be at their equilibrium values when evaluating these G-matrix elements. Such an approximation simplifies the treatment of the vibrations in CHD_3 and allows for a straightforward physical interpretation of the coupling of the C–H stretch to various normal modes.

The normal modes with possible coupling to the C–H stretching local mode in CHD_3 consist of two nondegenerate A_1 symmetry modes with harmonic frequencies $\omega_2 = 2185$ cm^{-1} and $\omega_3 = 1042$ cm^{-1} and three doubly degenerate E symmetry modes with frequencies $\omega_4 = 2337$ cm^{-1}, $\omega_5 = 1335$ cm^{-1}, and $\omega_6 = 1070$ cm^{-1}. These modes couple with varying degrees to the C–H stretching local mode as a result of the G-matrix terms in Eq. (3.3b).

Since a full matrix diagonalization of the Hamiltonian [Eq. (3.2)] in a suitable basis is impractical due to the large number of vibrational degrees of freedom in this molecule, a simpler, more transparent approach was taken to determine which modes couple strongly to the C–H stretch. This approach was to determine the strength of the coupling of the "pure" C–H stretching states $|v,0,...,0\rangle$ to resonant "doorway states"[4,9] such as $|v-1,v_2,v_3,...,v_9\rangle$. The degree to which two such zeroth order states mix was determined by simple diagonalizations of 2×2 matrices of the Hamiltonian [Eq. (3.2)] represented in this basis. For the nondegenerate A_1 symmetry normal mode states, a nondegenerate harmonic oscillator basis[19] was used, while, for the doubly degenerate E symmetry normal mode states, a doubly degenerate harmonic oscillator basis[19] was employed. The C–H stretching local mode basis states were taken to be Morse oscillator eigenfunctions.[17,18] The Morse oscillator matrix elements of the G-matrix coupling terms [Eq. (3.3b)] were calculated by numerical quadrature, rather than using the expansion employed in Refs. 4(a) and 7 of these terms in a Taylor series. It was found that this numerical integration avoided problems due to the slow convergence of the series expansion terms. Details of this integration procedure are described in Appendix A.

B. Vibrational analysis for CHD_3 and CHT_3

Two key features of the vibrational state mixing as described by pure G-matrix coupling are first summarized. They were investigated and found to simplify the analysis considerably:

(1) The two A_1 symmetry normal modes are rigorously decoupled from the C–H stretch because the G-matrix terms in Eq. (3.4) for these modes are independent of the C–H displacement coordinate r. While this behavior is not necessarily evident from Eq. (3.4), it may be shown by demonstrating the independence of the A_1 symmetry normal mode frequencies from the C–H bond length using standard normal mode techniques.[16]

(2) It is found in the calculations that the doubly degenerate E symmetry modes with harmonic frequencies $\omega_4 = 2337$ cm^{-1} and $\omega_6 = 1070$ cm^{-1} have extremely weak coupling to the C–H stretch via G-matrix terms. They also have no low order resonance condition with this mode for $v = 1$–6. Accordingly, coupling to these modes corresponds to effects of second order. For example, the states $|6\rangle|0,0\rangle_i$ and $|5\rangle|2,0\rangle_i$ (both of A_1 symmetry), where a doubly degenerate harmonic oscillator basis $|n,l\rangle_i$ is used for the particular E symmetry normal mode i, are coupled. However, the ratio of the matrix element that couples these two states (with $\hbar = 1$)

$$V_{12} = \omega_i \langle v-1|\tilde{G}_{i,i}(r)|v\rangle/2 \tag{3.7}$$

to the energy difference between them is straightforwardly calculated for $v = 6$ to be 0.002 for coupling to E mode 4 and 0.019 for coupling to E mode 6. Thus, these vibrational modes only weakly couple by G-matrix terms to the pure C–

H stretch and may be ignored in the present analysis.

The remaining doubly degenerate E symmetry normal mode is found in the calculations to be strongly coupled to the C–H stretch, with an average off-diagonal matrix element of the $\tilde{G}_{i,i}$ coupling term of $\sim 100\ \mathrm{cm}^{-1}$ in the range $v = 3$–6. Moreover, the harmonic frequency ω_5 of this normal mode satisfies a 1:2 nonlinear resonance condition with the C–H vibrational frequency at the $v = 5$ and 6 level of excitation. As a result, the states $|v\rangle|0,0\rangle$ and $|v-1\rangle|2,0\rangle$ in this energy regime are approximately degenerate in zeroth order. This bending mode involves the E symmetry deformation of the H–C–D angles and it thus interacts strongly with the C–H stretch via the curvilinear G-matrix coupling effect. The physical origin for this effect is due to the effective mass for the H–C–D bend, as described by the inverse of the G-matrix term, being increased when the local mode is excited and the C–H bond is lengthened. No other normal modes of the molecule satisfy both a low order resonance condition and the condition that the H–C–D bend be included in their motion.

One further possibility to be considered is the coupling of the pure C–H stretching state to A_1 symmetry combination states by terms like $\tilde{G}_{ij}(r)P_iP_j$ in Eq. (3.3b). These combination states have the form $|v-1,\ldots,v_i,v_j,\ldots\rangle$, where the normal mode quantum numbers other than v_i and v_j are zero. The combination state having $v_5 = 1$, $v_6 = 1$ is the only state found to have both an approximate zeroth order degeneracy and a nonnegligible interaction with the pure state $|v,0,0,\ldots\rangle$. In the calculations, it becomes important only for a level of excitation in the C–H oscillator corresponding to at least seven quanta in zeroth order. For six quanta in the C–H stretch, this combination state is sufficiently detuned from the C–H stretching state energy so as to have only a small second order effect on the splitting ($< 5\ \mathrm{cm}^{-1}$) and the relative intensity ($< 3\%$) of the Fermi resonance found in this spectral region.

The results of the above analysis indicate that the C–H stretch selectively interacts with the doubly degenerate bending normal mode with harmonic frequency $\omega_5 = 1335\ \mathrm{cm}^{-1}$, thereby simplifying the quantitative treatment of the C–H stretching states (i.e., only three degrees of freedom need be considered). However, since the magnitude of the pure curvilinear G-matrix interaction ($\sim 100\ \mathrm{cm}^{-1}$) is larger than what is observed experimentally ($\sim 35\ \mathrm{cm}^{-1}$), the potential energy is postulated to have an important cancellation effect within these matrix elements. Because the available high order force constants[20(a)] relevant to the Fermi resonances at $v = 5$ and 6 were found to be inadequate, only first order effects (in terms of degenerate perturbation theory) were treated. As will be shown later for CHD_3, this first order treatment is useful in determining both the energies and the relative intensities of the pure C–H stretching mode states and of combination levels involving the C–H stretch and the H–C–D bending mode.

The Hamiltonian for the coupled C–H stretch and doubly degenerate bending mode is

$$H = H_0 + V' \tag{3.8}$$

with

$$H_0 = H_m(r,p) + \tfrac{1}{2}[(P_1^2 + P_2^2) + \omega_5^2(Q_1^2 + Q_2^2)] \tag{3.9}$$

and

$$V' = \tfrac{1}{2}[\tilde{G}_{5,5}(r) - 1](P_1^2 + P_2^2) + \frac{F_3}{2} r(Q_1^2 + Q_2^2) + \frac{F_4}{4} r^2(Q_1^2 + Q_2^2), \tag{3.10}$$

where Q_1 and Q_2 are the degenerate pair of normal mode coordinates for the bending mode with conjugate momenta P_1 and P_2, $H_m(r,p)$ is the C–H stretch Morse oscillator Hamiltonian, and F_3 and F_4 are the cubic and quartic force constants, respectively, for the interaction of the C–H stretch with the bend.

The basis states of the zeroth order Hamiltonian [Eq. (3.9)] are the states $|v\rangle|n,l\rangle_5$, where $|v\rangle$ are the Morse oscillator eigenfunctions[18] for the C–H stretch and $|n,l\rangle_5$ is the doubly degenerate harmonic oscillator basis[19] for the ν_5 bending mode. The Fermi resonances in CHD_3 are presumed to involve the pure C–H stretching state $|v\rangle|0,0\rangle_5$ of A_1 symmetry interacting with the A_1 combination state $|v-1\rangle|2,0\rangle_5$. The relevant matrix elements for the bending normal mode are (in units of $\hbar = 1$)[19]:

$$\langle n,0|P_1^2 + P_2^2|n+2,0\rangle = (n+2)\omega_5/2, \tag{3.11a}$$

$$\langle n,0|Q_1^2 + Q_2^2|n+2,0\rangle = -(n+2)/(2\omega_5), \tag{3.11b}$$

$$\langle n,0|P_1^2 + P_2^2|n,0\rangle = (n+1)\omega_5, \tag{3.11c}$$

and

$$\langle n,0|Q_1^2 + Q_2^2|n,0\rangle = (n+1)/\omega_5. \tag{3.11d}$$

The 2×2 Fermi resonance matrix for this treatment is

$$\begin{pmatrix} H_{11} & H_{12} \\ H_{21} & H_{22} \end{pmatrix} = \begin{pmatrix} H_1 + V_{11} & V_{12} \\ V_{12}^* & H_2 + V_{22} \end{pmatrix}, \tag{3.12}$$

where (with $\hbar = 1$)

$$H_1 = (v - \tfrac{1}{2})\omega_1 - (v - \tfrac{1}{2})^2\omega_1\chi + 3\omega_5, \tag{3.13a}$$

$$H_2 = (v + \tfrac{1}{2})\omega_1 - (v + \tfrac{1}{2})^2\omega_1\chi + \omega_5, \tag{3.13b}$$

$$V_{11} = \frac{3\omega_5}{2}\langle v-1|[\tilde{G}_{5,5}(r) - 1]|v-1\rangle + \frac{3}{\omega_5}\left(\frac{F_3}{2}\langle v-1|r|v-1\rangle + \frac{F_4}{4}\langle v-1|r^2|v-1\rangle\right), \tag{3.13c}$$

$$V_{22} = \frac{\omega_5}{2}\langle v|[\tilde{G}_{5,5}(r) - 1]|v\rangle + \frac{1}{\omega_5}\left(\frac{F_3}{2}\langle v|r|v\rangle + \frac{F_4}{4}\langle v|r^2|v\rangle\right), \tag{3.13d}$$

and

$$V_{12} = \frac{\omega_5}{2}\langle v-1|\tilde{G}_{5,5}(r)|v\rangle - \frac{1}{\omega_5}\left(\frac{F_3}{2}\langle v-1|r|v\rangle + \frac{F_4}{4}\langle v-1|r^2|v\rangle\right). \tag{3.13e}$$

The Morse matrix elements of the normal mode-transformed G-matrix element $\tilde{G}_{5,5}(r)$ [Eq. (3.4)] were calculated

by numerical quadrature, as in Appendix A. The matrix elements of r and r^2, known analytically,[18,21] are discussed in Appendix B. Both the cubic and quartic terms, involving the Morse matrix elements $\langle v|r|v-1\rangle$ and $\langle v|r^2|v-1\rangle$, respectively, were found to be nonnegligible for $v=5$ or 6. The force constants in these terms were determined by a nonlinear least squares parameter fit[22] of the calculated values to the experimental data for $v=1$ through $v=6$. This fit was performed using a 2×2 matrix, as in Eq. (3.12), to calculate the energies of the C–H overtones and combinations at each energy level through $v=6$. Using a grid of values for F_3 and F_4, the minimum of the least squares function was found. Since only first order effects were considered in this treatment, the cubic and quartic force constants obtained in such an least squares analysis represent a first order estimate.

The kinetic and potential perturbation contributions to the diagonal elements in Eq. (3.12) also contributed in this calculation. The contribution from the G-matrix terms to the matrix elements V_{ii} represents, in effect, a modification of the bending mode's harmonic frequency ω_5,[23,24] namely,

$$H_{ii}=E_v^m+(n+1)\omega_5'+\langle v|V'_{\rm pot}|v\rangle, \tag{3.14a}$$

where

$$\omega_5'=\omega_5\left\{1+\frac{1}{2}\left[\langle v|\tilde{G}_{5,5}(r)|v\rangle-1\right]\right\} \tag{3.14b}$$

and E_v^m is the energy of the Morse oscillator with v quanta. Since the diagonal element $\langle v|\tilde{G}_{5,5}(r)|v\rangle$ is always less than unity (i.e., the effective mass of the bend increases with increasing v), the effective harmonic frequency ω_5' of the bending mode decreases with increasing v. For the CHD_3 molecule, the potential energy term has a similar effect except that it is somewhat more complicated in form. Both contributions give rise, as a result, to an effective anharmonicity for the C–H overtones.[23,24] For the point of view of that interpretation, the values of ω_1 and $\omega_1\chi$ taken from experimentally measured Birge–Sponer lines may deviate somewhat from the "true" Morse parameters for the C–H mode, as is shown later for CHD_3.

The effect of the coupling of the above $|v-1\rangle|2,0\rangle_5$ states to A_1 symmetry states like $|v-2\rangle|4,0\rangle_5$, with four quanta in the bending mode, was also examined. These couplings can, in principle, have a large effect, as was suggested recently for benzene.[4] In the case of CHD_3, however, these states are strongly detuned from the principal Fermi resonance due, in part, to the diagonal first order energy corrections just mentioned [Eqs. (3.14a) and (3.14b)]. Moreover, these states seem to be particularly sensitive to second order corrections from off-resonant states such as $|v-1\rangle|4,0\rangle_5$ or $|v-3\rangle|4,0\rangle_5$. These corrections tend to lower the energy of these states even more so that they are further detuned from the principal Fermi resonance.

To explore such effects, diagonalizations of 27×27 secular determinants for the Hamiltonian [Eq. (3.8)], including states with four quanta in the bending mode and as many as nine C–H stretching quanta, were performed. Since it is computationally expensive to use a 27×27 matrix diagonalization in the determination of the force constants F_3 and F_4 by the nonlinear least squares fitting procedure described previously, two separate approaches to this problem were taken. The first approach was to determine the values of F_3 and F_4 using a 2×2 matrix such as Eq. (3.12) at each level of C–H excitation ($v=1$–6) in conjunction with the force constant fitting procedure discussed previously. A 27×27 matrix was subsequently diagonalized utilizing the force constants thus obtained. The second approach was to extend the nonlinear least squares fitting procedure to include the diagonalization of a 3×3 matrix (including the states with four bending quanta) at each level of C–H excitation. The force constants obtained in this fit were then used in a diagonalization of a 27×27 secular determinant.

The results of all four calculations are shown in Table II together with the experimental values. It is evident that the results for the simple 2×2 treatment and the subsequent 27×27 diagonalization are consistent with the experimental values and with each other (i.e., the results do not differ significantly between the 2×2 and the 27×27 treatment). Interestingly enough, as one can see from Table II, the 3×3 treatment does not fit the experimental data as well nor are the 3×3 results consistent with the subsequent 27×27 matrix diagonalization using those parameters. These results indicate that the simple 2×2 procedure is the best way to fit the experimental data.

Both 27×27 matrix diagonalizations exhibit the strong second order detuning effect of the $|v-2\rangle|4,0\rangle_5$ states mentioned previously. For the diagonalization utilizing the parameters obtained from the 2×2 fitting procedure, this energy shift for the $v=6$ region was estimated from second order nondegenerate perturbation theory to be

$$\Delta^{(2)}=\frac{|V_{12}|^2}{E_1^{(0)}-E_2^{(0)}}+\frac{|V_{13}|^2}{E_1^{(0)}-E_3^{(0)}}\simeq-80\ \text{cm}^{-1},$$

TABLE II. Comparison of theoretical results.

	$v=5$ splitting[c] (cm^{-1})	$v=6$ splitting[c] (cm^{-1})	$v=5$ rel. intensity	$v=6$ rel. intensity
Expt.	133	74	$18\pm8\%$	$55\pm10\%$
2×2	117	79	9%	43%
27×27[a]	131	78	7%	40%
3×3	99	59	13%	97%
27×27[b]	138	84	7%	25%

[a] Calculated using parameters from 2×2 fit.
[b] Calculated using parameters from 3×3 fit.
[c] Fermi resonance splittings between eigenstates of $|v\rangle|0,0\rangle$ and $|v-1\rangle|2,0\rangle$ parentage.

TABLE III. Molecular parameters for $CHD_3(CHT_3)$.

	Morse harmonic freq. $\omega_1(cm^{-1})$[a]	Morse anharmonicity $\omega_1\chi(cm^{-1})$[b]	ν_5 mode harmonic freq. (cm^{-1})[c]	Cubic force constant F_3 (a.u.)[d]	Quartic force constant F_4 (a.u.)[d]
CHD_3	3133	58.08	1335	-2.03×10^{-5}	1.83×10^{-5}
CHT_3	3133	58.08	1273	-1.82×10^{-5}	1.64×10^{-5}

[a] From Ref. 20(a).
[b] From Ref. 25.
[c] Calculated from the quadratic force constants given in Ref. 20(a).
[d] As determined from least squares parameter fit.

where 1 denotes the state $|4\rangle|4,0\rangle_5$, 2 denotes the state $|5\rangle|4,0\rangle_5$, and 3 denotes the state $|3\rangle|4,0\rangle_5$. The exact 27×27 treatment, in this case, has a shift for this state of $\simeq -120\,cm^{-1}$ instead of $-80\,cm^{-1}$. Due to this detuning effect, we conclude that the states with four quanta in the bend are not important to the observed Fermi resonances.

C. Results for CHD_3

The energies of the C–H stretch overtones for CHD_3, as calculated from the 2×2 fitting procedure given in Sec. III B and utilizing the molecular parameters from Table III, are compared with the experimental results in Table IV. The results are in good agreement with experiment for both the pure C–H stretching states and the combination levels. The corresponding theoretical least squares Birge–Sponer line (in cm^{-1}) through the $v=6$ overtone is given by $\Delta E_{ov}/v = 3047 - 57.56v$. This line was determined by using a linear least squares fit to the calculated points for $v=1$ through 4 and fits the theoretical data very well except at $v=5$ and 6, where a deviation is expected due to the onset of the Fermi resonances. As compared with Ref. 25, where a fit was obtained for the $v=1$–4 C–H overtones, there is, from a phenomenological point of view, two new pieces of experimental data, namely the splittings at $v=5$ and 6, and two new parameters introduced into the fit. Of course, this does not require that the model will automatically fit the data, but it does nevertheless. The main virtue, we believe, of the present analysis is that it describes the physics of the problem. In particular, it is found that the treatment of the dynamical (i.e., G-matrix) coupling does not quantitatively explain the Fermi resonances, i.e., the force constants F_3 and F_4 should be included. Such force constants are ultimately to be compared with *ab initio* calculations. Other treatments which either do not employ curvilinear coordinates and/or potential energy contributions of cubic order or higher can be considered to be more phenomenological.

In Table V, the relative intensities for the two Fermi resonances at $v=5$ and $v=6$ are listed along with the off-diagonal matrix elements and the detunings of the diagonal matrix elements. In calculating these relative intensities, the dipole moment for the C–H stretching transitions was assumed to be a function of only the C–H oscillator coordinate r.[1(c)] As a result, the relative intensity of the two states involved in the Fermi resonance is determined by the overlap of the zeroth order pure C–H stretching state with the actual eigenstates. The relative intensity is thus defined as

$$I_r = (b/a)^2\times100\%, \tag{3.15}$$

where

$$a = |\langle v,0|\psi_0\rangle|, \quad b = |\langle v,0|\psi_2\rangle|. \tag{3.16}$$

Here, $|v,0\rangle$ denotes the zeroth order pure C–H stretching state $|v\rangle|0,0\rangle_5$, ψ_0 is the eigenstate of $|v\rangle|0,0\rangle_5$ parentage, and ψ_2 is the eigenstate of $|v-1\rangle|2,0\rangle_5$ combination state parentage. These relative intensities in Table V are in reasonable agreement with the experimental results, but the discrepancy is larger than that for the splittings. This discrepancy may reflect slight inaccuracies in the zeroth order detunings and/or off-diagonal electrical anharmonicity terms contained in the actual dipole moment function. A theoretical spectrum (at $v=6$) employing the above results

TABLE IV. Energies of C–H overtones and combinations for $CHD_3(CHT_3)$.

State[a]	CHD_3 expt.[b] (cm^{-1})	CHD_3 calc. (cm^{-1})	CHT_3 calc. (cm^{-1})
$\|1,0\rangle$	2 992	2 990	2 990
$\|2,0\rangle$	5 865	5 864	5 865
$\|3,0\rangle$	8 623	8 624	8 624
$\|4,0\rangle$	11 267	11 269	11 269
$\|4,2\rangle$	13 668	13 684	13 558
$\|5,0\rangle$	13 801	13 801	13 800
$\|5,2\rangle$	16 156	16 149	16 029
$\|6,0\rangle$	16 230	16 228	16 218

[a] Refers to the zero-order parentage of the state. This notation denotes the states $|v\rangle|n,0\rangle$ (with $l=0$ in all cases).
[b] Taken from Ref. 2.

TABLE V. Relative intensities, off-diagonal matrix elements, and diagonal detunings[a] for CHD_3 and CHT_3.

Molecule and energy level	Expt. relative intensity[b]	Calc. relative intensity	Off diagonal matrix element V_{12} (cm^{-1})	Diagonal detuning δ (cm^{-1})
CHD_3 $v=5$	$18 \pm 8\%$	9%	−32	98
CHT_3 $v=5$	...	4%	−47	223
CHD_3 $v=6$	$55 \pm 10\%$	43%	−36	31
CHT_3 $v=6$	...	9%	−52	159

[a] The diagonal detuning is defined from Eq. (3.12) as $\delta = (H_2 + V_{22}) - (H_1 + V_{11})$.
[b] Taken from Ref. 2.

and the measured excited state rotational constants from Ref. 2 is shown in Fig. 3. The main discrepancy with the experimental spectrum (shown in Fig. 1) is due to the differences in the relative intensities.

The diagonal first order perturbation contributions [Eq. (3.13d)] to the pure C–H stretching energies are given in Table VI. One sees that, according to the results, these terms contribute even for the fundamental transition. Furthermore, the G matrix and the potential energy contributions are of comparable magnitude for all excitations. Indeed, the effective Morse parameters $\omega_1 = 3105$ cm^{-1} and $\omega_1\chi = 57.56$ cm^{-1} calculated from the theoretical Birge–Sponer line for CHD_3 are quite different from the actual values given for the Morse oscillator in Table III. This difference reflects the diagonal first order perturbation effect. Thus, as noted before, parameters for the C–H bond Morse oscillator potential functions obtained from experimental Birge–Sponer plots should be used with this in mind: they are effective parameters.

The procedure used for calculating the C–H overtones and Fermi resonance combinations was extended to the $v = 7$ region where now both the ν_5 and ν_6 modes couple to the C–H stretch. A 3×3 matrix was used with the zeroth order A_1 symmetry basis states (with energies $E_{c^0} < E_{b^0} < E_{a^0}$)

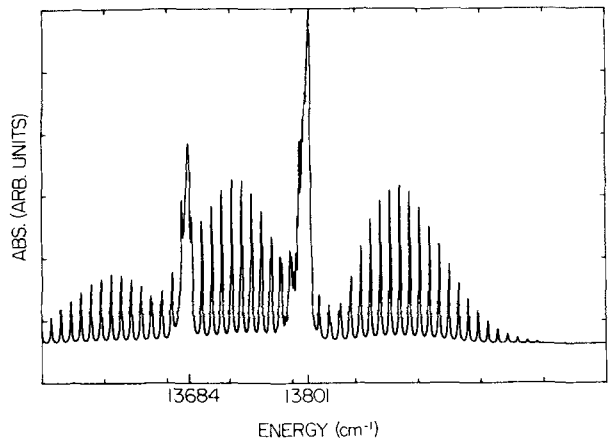

FIG. 3. Theoretical $v = 6$ C–H overtone spectrum for CHD_3.

$$|a^0\rangle = |6\rangle|2,0\rangle_5|0,0\rangle_6, \tag{3.17a}$$

$$|b^0\rangle = |7\rangle|0,0\rangle_5|0,0\rangle_6, \tag{3.17b}$$

$$|c^0\rangle = |6\rangle\left[\frac{1}{\sqrt{2}}(|1,-1\rangle_5|1,1\rangle_6 + |1,1\rangle_5|1,-1\rangle_6)\right], \tag{3.17c}$$

where the notation $|v\rangle|n,l\rangle_5|n',l'\rangle_6$ represents the Morse oscillator eigenket for the C–H mode, the $|n,l\rangle$ eigenket for the fifth normal mode ($\omega_5 = 1335$ cm^{-1}), and the $|n,l\rangle$ eigenket for the sixth normal mode ($\omega_6 = 1070$ cm^{-1}), respectively. The term

$$V_{56} = \tilde{G}_{56}(r)(P_{5,1}P_{6,1} + P_{5,2}P_{6,2}) + F_{56}r(Q_{5,1}Q_{6,1} + Q_{5,2}Q_{6,2}) \tag{3.18}$$

was added to the perturbation given in Eq. (3.10).[20(b)] This perturbation term is responsible for the coupling of the $|c^0\rangle$ state to the $|a^0\rangle$ and $|b^0\rangle$ states. The subscripts 5 and 6 have been added here to distinguish between the two normal modes while, as before, the subscripts 1 and 2 in Eq. (3.18) refer to the degenerate pairs of coordinates and momenta for these vibrations. Diagonalization of the 3×3 matrix gave perturbed states $|a\rangle$, $|b\rangle$, and $|c\rangle$ with splittings $\Delta_{bc} \sim 110$ cm^{-1} and $\Delta_{ab} \sim 55$ cm^{-1}. The experimental results from Ref. 2 give splittings of ~ 120 and ~ 60 cm^{-1}, respectively. No quantitative comparison of the relative intensities could be made since they were not obtained experimentally for this level. Nevertheless, the theoretical results suggest that the intensity may be distributed approximately uniformly over the three levels in qualitative agreement with what may be seen from visual inspection of the spectrum at $v = 7$.[2]

D. Results for CHT_3

The theoretical treatment of Sec. III A for the $v = 1$–6 transitions in CHD_3 was applied to CHT_3 to investigate the effect of the isotopic substitution D to T. It was again concluded that the fifth normal mode is the only vibration interacting strongly with the C–H stretch by G-matrix coupling and that the simplified treatment of Sec. III B may be applied to CHT_3. The cubic and quartic force constants found

TABLE VI. Calculated first order diagonal corrections to the local mode states in CHD_3.

Zero-order local mode state v	$\tilde{G}$-matrix contribution (cm^{-1})	Potential energy contribution (cm^{-1})	Total correction (cm^{-1})
1	−20	−21	−41
2	−34	−35	−69
3	−48	−47	−95
4	−62	−59	−121
5	−76	−69	−145
6	−90	−78	−168

for CHD_3 were transformed to the CHT_3 normal mode coordinate system with the aid of the transformation in Appendix C. The results for the energies are given in Table IV. The relative intensities of the Fermi resonances, the off-diagonal matrix elements, and the detunings of the diagonal matrix elements are given in Table V. This model predicts significantly less intensity sharing by the combination states in the $v = 5$ and 6 regions than in CHD_3 due to a detuning of the Fermi resonance: the fifth normal mode for CHT_3 has a harmonic frequency of only $\omega_5 = 1273\ cm^{-1}$ as opposed to 1335 cm^{-1} for CHD_3. This effect far outweighs the contribution due to the increased magnitude of the off-diagonal matrix element (as seen in Table V) and results in a much "purer" C–H stretching state at $v = 5$ and 6.

This analysis of CHT_3 raises two interesting questions. First, the density of vibrational states would obviously be higher for CHT_3 than for CHD_3. Thus, CHT_3 presents a case in which the experimental verification of the results predicted by this model would indicate that the density of states need not predominate in determining the degree of state mixing in structually similar molecules. Rather, the degree of mixing of states may be determined primarily by a specific physical mechanism, as in the case of CHD_3. Second, CHT_3 has the possibility of having 1:3 nonlinear resonance conditions between the C–H stretch, an A_1 mode ($\omega_3 = 905\ cm^{-1}$), or a doubly degenerate E mode ($\omega_6 = 900\ cm^{-1}$). This resonance condition is possible around the $v = 3$ or 4 level of excitation in the C–H mode. However, the sixth mode involves almost entirely T–C–T bending and C–T stretching motions and so is not expected to be physically coupled to the C–H stretch. The third mode, on the other hand, involves both the H–C–T and the T–C–T bending, but, as was found for the A_1 symmetry modes in CHD_3, it has no G-matrix element providing coupling to the C–H stretch. In addition, the resonant $|v-1,3\rangle_i$ states of either mode cannot couple directly to the pure C–H stretching states via the perturbation terms like those given in Eq. (3.10) as long as the harmonic oscillator basis is a good one for those normal modes. Experimental observation of significant 1:3 Fermi resonances in this molecule would indicate that the simple theoretical/physical picture presented in Eqs. (3.8)–(3.13e) needs extension. Possible extensions include a dynamical dependence of the G-matrix term in Eq. (3.10) on the normal mode Q_6 or the presence of significant fourth order force constants proportional to rQ_3^3 or rQ_6^3 in the potential energy function.

A curvilinear coordinate treatment is next used to estimate the vibrational state mixing in CH_3D.

IV. THEORY FOR CH_3D

A. Vibrational analysis

The CH_3D molecule has three equivalent C–H oscillators, so it is useful to prediagonalize the CH_3 local mode problem[1] before treating the interactions of these modes with the bending normal modes. The properly symmetrized zeroth order local mode basis states for C_{3v} symmetry were found using the method of Halonen and Child.[21,25] For the sake of brevity, these basis states are not presented here, but they consist in general of the A_1, A_2, E_a, and E_b linear combinations of different permutations of the unsymmetrized local mode state

$$|v_1,v_2,v_3\rangle, \tag{4.1}$$

where the subscripts 1, 2, and 3 refer to the Morse oscillator basis states for the three C–H bonds. The corresponding C–H local mode Hamiltonian is

$$H_m = H_m^0 + V_m', \tag{4.2}$$

where

$$H_m^0 = \sum_i^3 H_i(p_i,r_i) \tag{4.3}$$

and

$$V_m' = \sum_{i>j}^3 G_{ij}\, p_i\, p_j + \sum_{i>j}^3 F_{ij} r_i\, r_j, \tag{4.4}$$

and may be diagonalized in the symmetrized local mode basis. In these equations, $H_i(p_i,r_i)$ is a Morse oscillator Hamiltonian with curvilinear bond displacement coordinate r_i and conjugate momentum p_i; G_{ij} and F_{ij} are the off-diagonal G-matrix element and the off-diagonal quadratic force constant, respectively, for two C–H stretching local modes i and j. The G-matrix element used in this calculation may be found analytically,[16] the quadratic stretch–stretch interaction force constant was obtained from the Gray and Robiette potential energy surface,[20(c)] and the Morse parameters are the same as those used for CHD_3 (Table III). The eigenvalues and eigenfunctions of this Hamiltonian were calculated for manifolds with $v = 4$, 5, and 6 total quanta in the C–H stretches.[21,25] Couplings by the perturbation term (4.4) between manifolds of states with different total v were neglected since they are far off resonance. Each manifold of states has four independent blocks of A_1, A_2, E_a, and E_b symmetry, and the properly symmetrized "pure" local mode states (i.e., symmetrized linear combinations of $|v,0,0\rangle$) are nearly degenerate for all blocks that included such states (there is one pure state each in the A_1, E_a, and E_b blocks).

The interaction of the prediagonalized local mode

states with the bending degrees of freedom was next calculated. This step is usually omitted in the customary local mode treatment[1,21,25] but, as was learned in the CHD_3 analysis, is useful in understanding the breakdown of localized C–H stretching vibrations. As a first step, the interaction of the CH_3 local modes with the bending vibrations was calculated using only the G-matrix coupling technique presented in Sec. III A. Due to the limited experimental resolution of individual vibrational lines at $v = 6$ in this molecule, a treatment of the potential energy contributions to the state coupling was not attempted.

The description of the normal modes was made by performing a standard normal mode analysis[16] on the quadratic Hamiltonian

$$H_N = \frac{1}{2}\sum_{i,j}' G_{ij}(\mathbf{x}_0)p_i\,p_j + \frac{1}{2}\sum_{i,j}' F_{ij}q_iq_j, \tag{4.5}$$

where the primes on the summations indicate a summation over all internal symmetry coordinates q_i (see Table VII) other than the three C–H stretching coordinates. This treatment defines three normal modes with harmonic frequencies $\omega_3 = 1366\ \text{cm}^{-1}$, $\omega_5 = 1524\ \text{cm}^{-1}$, and $\omega_6 = 1222\ \text{cm}^{-1}$ that are in approximate 1:2 nonlinear resonance with the C–H stretches. The fifth and sixth vibrations are both doubly degenerate modes of E symmetry while the third vibration is the A_1 symmetry umbrella mode.[20(a)] As for CHD_3, the C–H stretching coordinates are treated separately when defining the zeroth order oscillator basis.

The curvilinear Hamiltonian used for this problem, containing the third, fifth, and sixth normal modes and the C–H local modes, is

$$H = H_0 + V' + V_d, \tag{4.6a}$$

where

$$\begin{aligned} H_0 = H_m &+ \frac{1}{2}(P_3^2 + \omega_3^2 Q_3^2) \\ &+ \frac{1}{2}[(P_{5,1}^2 + P_{5,2}^2) + \omega_5^2(Q_{5,1}^2 + Q_{5,2}^2)] \\ &+ \frac{1}{2}[(P_{6,1}^2 + P_{6,2}^2) + \omega_6^2(Q_{6,1}^2 + Q_{6,2}^2)], \end{aligned} \tag{4.6b}$$

$$V' = \frac{1}{2}[\tilde{G}_{3,3}(r_1,r_2,r_3) - 1]$$

TABLE VII. Internal symmetry coordinates for CH_3D.[a]

$$\begin{aligned} q_1 &= r \\ q_2 &= r_1 \\ q_3 &= r_2 \\ q_4 &= r_3 \\ q_5 &= \frac{1}{\sqrt{6}}(\alpha_1 + \alpha_2 + \alpha_3 - \beta_1 - \beta_2 - \beta_3) \\ q_6 &= \frac{1}{\sqrt{6}}(2\alpha_1 - \alpha_2 - \alpha_3) \\ q_7 &= \frac{1}{\sqrt{6}}(2\beta_1 - \beta_2 - \beta_3) \\ q_8 &= \frac{1}{\sqrt{2}}(\alpha_2 - \alpha_3) \\ q_9 &= \frac{1}{\sqrt{2}}(\beta_2 - \beta_3) \end{aligned}$$

[a] The coordinates are defined the same way as in Table I except that r is now the C–D displacement coordinate and r_i is a C–H displacement coordinate.

$$\begin{aligned} &+ \frac{1}{2}\sum_{n=1}^{2}[\tilde{G}_{5,5;n}(r_1,r_2,r_3) - 1]P_{5,n}^2 \\ &+ \frac{1}{2}\sum_{n=1}^{2}[\tilde{G}_{6,6;n}(r_1,r_2,r_3) - 1]P_{6,n}^2 \\ &+ \sum_{n=1}^{2}\tilde{G}_{5,6;n}(r_1,r_2,r_3)P_{5,n}\,P_{6,n}, \end{aligned} \tag{4.6c}$$

and the diagonal matrix element of the V_d potential energy term is written as

$$\langle v_3|V_d|v_3\rangle = -(v_3 + \tfrac{1}{2})^2\omega_3\chi_3. \tag{4.6d}$$

Here, H_m is the C–H local mode Hamiltonian from Eq. (4.2), $\tilde{G}_{3,3}(r_1,r_2,r_3)$ is the normal mode transformed G-matrix element [Eq. (3.4)] for the nondegenerate A_1 mode, $\tilde{G}_{i,i;n}(r_1,r_2,r_3)$ is the normal mode transformed G-matrix element for doubly degenerate normal mode i with degenerate partner n, and $\tilde{G}_{5,6;n}(r_1,r_2,r_3)$ is the G-matrix cross term for the degenerate normal modes 5 and 6 and degenerate partner n. All of these G-matrix elements are assumed to depend only on the three C–H bond lengths r_1, r_2, and r_3. This approximation is analogous to the one made for CHD_3, where the C–H mode was taken to be the only vibration with appreciable amplitude. The $|v_3\rangle$ ket denotes a vibrational state of the A_1 mode such that $\langle v_3|V_d|v_3\rangle$ has the effect of a diagonal anharmonicity with the adjustable anharmonicity parameter $\omega_3\chi_3$. The work of Gray and Robiette[20(a)] suggests that this anharmonicity is significant and should not be neglected; an approximate value of $20\ \text{cm}^{-1}$ was chosen for this parameter. The other matrix elements of this vibrational mode are still treated in the harmonic limit, however, because this anharmonicity is not large enough to cause significant deviations from harmonic oscillator values.

The basis states defined by the zeroth order Hamiltonian [Eq. (4.6b)] are

$$|\psi\rangle = |v,j,\Gamma\rangle|v_3\rangle|n_5,l_5\rangle|n_6,l_6\rangle, \tag{4.7}$$

where $|v,j,\Gamma\rangle$ represents the jth eigenket (ordered by increasing energy) of the prediagonalized CH_3 local mode Hamiltonian H_m [Eq. (4.2)] from the manifold with v total C–H stretching quanta and symmetry Γ. Also, $|v_3\rangle$ is the nondegenerate harmonic oscillator basis for the third mode and $|n_i,l_i\rangle$ is the doubly degenerate harmonic oscillator basis for the fifth and sixth modes.

The matrix elements for the doubly degenerate bending modes were calculated in the same way as those for CHD_3/CHT_3 [Eqs. (3.10a)–(3.10c)] while the nondegenerate matrix elements were calculated from standard harmonic oscillator formulas.[19] The matrix elements

$$\langle v',j',\Gamma|\tilde{G}_{i,i;n}(r_1,r_2,r_3)|v,j,\Gamma\rangle, \tag{4.8}$$

in the prediagonalized local mode basis set $|v,j,\Gamma\rangle$, were nontrivial and could have required copious quantities of computer time. Several simplifications which made the evaluation of Eq. (4.8) tractable are given in Appendix D.

B. Results for CH_3D

In the notation of Eq. (4.7), the pure local mode state for $v = 6$ is

$$|\psi_1\rangle = |6,1,\Gamma\rangle|0\rangle|0,0\rangle|0,0\rangle, \tag{4.9}$$

where $|v,1,\Gamma\rangle$ is defined as the symmetrized state of pure local mode parentage and of Γ symmetry. These pure states are always lowest in energy within a manifold with v total quanta [i.e., in the notation of Eq. (4.7), they are denoted by $j=1$]. The only zeroth order states with less than or equal to four quanta in the bending modes found in the calculations to strongly interact by G-matrix coupling with this state are

$$|\psi_2\rangle = |5,1,\Gamma\rangle|2\rangle|0,0\rangle|0,0\rangle, \tag{4.10a}$$

$$|\psi_3\rangle = |5,1,\Gamma\rangle|0\rangle|0,0\rangle|2,0\rangle, \tag{4.10b}$$

and

$$|\psi_4\rangle = |4,1,\Gamma\rangle|4\rangle|0,0\rangle|0,0\rangle, \tag{4.10c}$$

where Γ denotes states of A_1, E_a, or E_b symmetry. In the calculations, it was also found that no states from Eq. (4.7) containing local mode combination states[1] are found to mix to any appreciable extent with the states (4.9) and (4.10a)–(4.10c) when the full matrix diagonalization (including the bending degrees of freedom) is performed.

An approximate theoretical spectral envelope was calculated for the $v=6$ overtone of CH_3D at 300 K (see Fig. 4). Standard selection rules for parallel and perpendicular type vibrational/rotational transitions in symmetric top molecules were used.[14] Moreover, as in the case of CHD_3, the body fixed C–H stretching dipole moment operator was assumed to have the form[1,21]

$$\mu(\mathbf{r}) = \sum_{i=1}^{3} \mu(r_i)\mathbf{e}_{r_i}, \tag{4.11}$$

where $\mathbf{e}_{r_i}$ is a unit vector directed along the ith C–H bond. The overlaps of the molecular eigenstates with the zeroth order pure C–H stretching state thus determine the relative intensities of the vibrational transitions. For Fig. 4, the individual vibrational/rotational lines were given a Lorentzian shape with a width at half-maximum of 1 cm^{-1}, as was determined experimentally.[2] A value of -0.2 cm^{-1} was assumed for the ground to excited state rotational constant difference $\Delta B = (B_v - B_0)$, representing a crude estimate of the change in the rotational constant in going to the excited state. The overall spectral envelope is not particularly sensitive to changes in the value of this parameter.

When compared with the experimental spectrum in Fig. 2, two features of the theoretical spectral envelope in Fig. 4 are immediately apparent. First, the two main peaks of the experimental envelope presumably correspond to states of zeroth order parentage $|6,1,\Gamma\rangle|0\rangle|0,0\rangle|0,0\rangle$ for the eigenstate to higher energy and $|5,1,\Gamma\rangle|0\rangle|0,0\rangle|2,0\rangle$ for the eigenstate to lower energy, with an experimental splitting of ~ 60 cm^{-1}. The theoretical spectrum has these same states present with a splitting of ~ 50 cm^{-1}. Moreover, the relative heights of the two peaks seem to be in qualitative agreement for the two spectra. A second feature is that the theoretical spectrum is noticeably less congested than the experimental one. We have considered the Coriolis interactions among only the pure local mode states and found them to be very ineffective in contributing to the observed spectral congestion (Appendix E).

For the theoretical spectrum at $v=6$ shown in Fig. 5, a Lorentzian line shape for each vibrational/rotational transition with a width of 30 cm^{-1} was assumed and is much closer in appearance to the experimental one. If one assumes a high degree of level mixing of the ro-vibrational states at $v=6$, then the "Golden Rule" formula $(2\pi/\hbar)\langle V\rangle^2\rho_{rv}$ may be used for the rate constant k for decay of the excitation. The homogeneous linewidth $\Delta\bar{\nu}$ is then given by $k/2\pi c$,[26] where c is the speed of light. Using the expression $(2J+1)\rho_v(\Gamma)$ for the average density of ro-vibrational states ρ_{rv} with symmetry Γ and rotational quantum number J,[27] typical values of the effective coupling element $\langle V\rangle$ needed to give linewidths of 30 cm^{-1} are found to be on the order of 0.1–1.0 cm^{-1}, depending on the value of J and the symmetry Γ. (Note the difference in magnitude of these matrix elements coupling to individual bath states as compared to those coupling the stretch to the bend in CHD_3). In these calculations, values of 1.85, 1.85, and 7.40 states/cm^{-1} were used for the density $\rho_v(\Gamma)$ of A_1, A_2, and E symmetry vibrational states, respectively, at the energy of the $v=6$ transition.[15] Whether the physical origin of the extra broadening in Fig. 5 is due to higher order potential energy and/or Coriolis interactions is at present not known. It should, however,

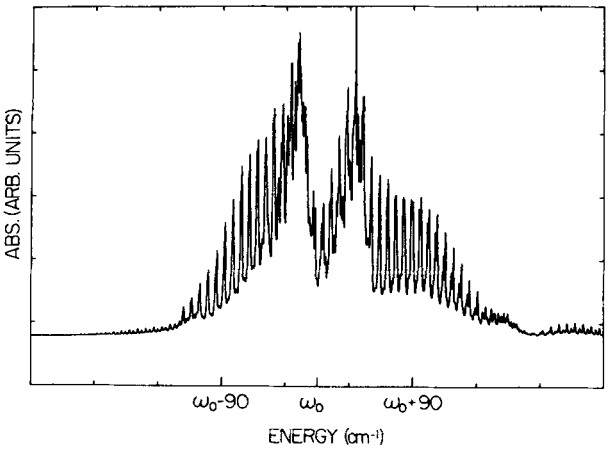

FIG. 4. Theoretical C–H overtone spectrum for CH_3D. The rotational contours were calculated using the rotational constants $B \simeq 3.88$ cm^{-1} and $A \simeq 5.25$ cm^{-1} [Ref. 20(a)] and the excited state rotational constant difference $\Delta B \simeq -0.2$ cm^{-1}. The individual vibrational/rotational transitions were given a Lorentzian line shape with a width at half-maximum of 1 cm^{-1}.

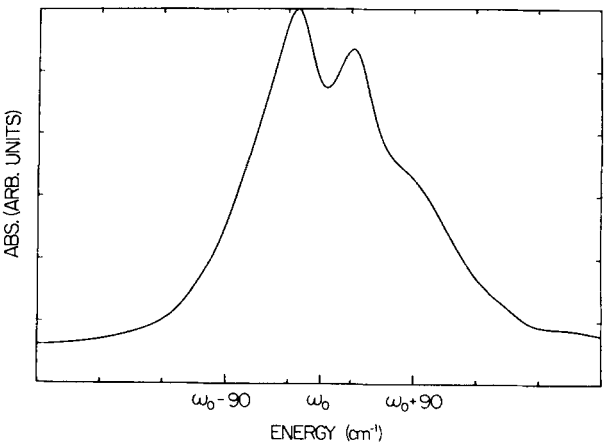

FIG. 5. Theoretical C–H overtone spectrum for CH_3D including a broadening of 30 cm^{-1} for each vibrational/rotational transition.

be mentioned that thermal congestion may be the source of the observed broadening in this molecule provided there are small but not negligible Coriolis interactions.

V. CONCLUDING REMARKS

In this paper, a theoretical analysis of the C–H stretching vibrations in CHD_3, CHT_3, and CH_3D was performed. The various coupling mechanisms in these molecules resulting from dynamical and, in the case of CHD_3 and CHT_3, potential energy interactions were considered. For CHD_3, the simplicity of the observed C–H overtone spectrum was qualitatively explained by treating the curvilinear G-matrix coupling[4] of the C–H stretch with the other vibrational normal modes, but this coupling is seen to be too large to quantitatively explain the Fermi resonances with the ν_5 mode. Potential energy contributions are therefore assumed to contribute a cancellation effect within the interaction matrix elements between zeroth order states. It was further concluded that the existence of a low order resonance condition between the C–H stretch and the other vibrations was crucial in determining the degree of vibrational mode coupling in these molecules. In CHD_3, it was deduced from the calculations that the C–H stretching local mode selectively interacts by these mechanisms with only one doubly degenerate normal mode involving D–C–H bending. Another approach to the present problem is the rectilinear coordinate method used by Quack *et al.*[28,29] for the C–H stretching states in the CHX_3 species (where X = D, F, etc.).

Predictions for CHT_3 are also presented, using the same model as for CHD_3, the only difference being in the normal mode frequencies due to the isotopic substitution D to T. The predictions of this model indicate the existence of a purer C–H stretching mode than was found for CHD_3 because the 1:2 resonance condition between the C–H stretch and the bend is detuned upon isotopic substitution. It is suggested that more subtle vibrational state mixing effects such as higher order resonances with other normal modes, weak potential energy couplings, and a higher density of states may be present in this molecule, although our model indicates that these are not important. The results presented in this paper for CHD_3 and CHT_3, together with the work of Sibert *et al.*[4] on the benzene local modes suggests it is possible that many intermediate and large size molecules may exhibit interesting behavior that only the detailed examination of the vibrational state coupling can reveal. One possibility is that certain molecular systems may be thought of as decoupled or very weakly coupled subsets of strongly interacting vibrational modes. There are implications of this picture for vibrational energy redistribution[12] and laser selective chemistry.[13] In fact, the results presented here are consistent with the recent observation in anthracene[30] of simple quantum beats, indicating that only a few (~ 3) levels are involved in the coupling even though the total density of states is quite high.

For CH_3D, it is found that the pure C–H stretching local modes do, in fact, mix to a greater degree by G-matrix coupling with bending normal modes than was found in CHD_3. It was also shown that local mode combination states[1] were not significantly coupled to these pure local modes. Thus, the present model suggests that the energy flow from an initially excited zeroth order nonstationary state like Eq. (4.9) would go almost exclusively into the bending degrees of freedom coupled to the C–H stretches and not into local mode combination states. This picture is similar to that presented by several authors[4,9] for C_6H_6.

While the calculated spectral envelope (Fig. 4) for CH_3D is congested due to vibrational/rotational transitions, we were unable to explain the observed high degree of spectral congestion (see Fig. 2) using pure G-matrix coupling effects. Potential energy or Coriolis couplings between the rovibrational states may be responsible for the added degree of congestion observed experimentally in this molecule.

ACKNOWLEDGMENTS

This work is supported by grants from the National Science Foundation. We would like to thank Dr. J. W. Perry for many helpful discussions on the experimental and theoretical aspects of this work and Dr. A. G. Robiette for information on the various coordinate systems used in our calculations.

APPENDIX A: INTEGRATION OF THE $\tilde{G}$ MATRIX ELEMENTS FOR CHD_3, CHT_3

The matrix elements $\langle v|\tilde{G}_{5,5}(r)|v'\rangle$ appearing in Eqs. (3.7) and (3.13c)–(3.13e) were calculated as follows: Computer subroutines were written (1) to calculate the G matrix[16] for a general tetrahedral molecule, the input parameters being the atomic masses and the bond lengths; (2) to calculate the normal mode matrix $\mathbf{L}^{-1}$ for all the displacement coordinates at their equilibrium value; (3) to perform the symmetry coordinate transformation [Eq. (3.5)] and the normal mode transformation [Eq. (3.4)]; (4) to calculate the value of the integrand $\psi_v^*(r)\tilde{G}_{5,5}(r)\psi_{v'}(r)$ from the matrix element $\langle v|\tilde{G}_{5,5}(r)|v'\rangle$ for an arbitrary value of the C–H bond displacement coordinate r, ψ_v and $\psi_{v'}$ being the Morse oscillator eigenfunctions[17,18]; and (5) to numerically integrate the integral $\langle v|\tilde{G}_{5,5}(r)|v'\rangle$ using Gaussian quadrature[31] for the classically allowed region and Laguerre quadrature[31] for the classically unallowed region. These subroutines were linked into a main computer code such that a value of $\tilde{G}_{5,5}(r)$ could be calculated at each r and the numerical integration in Eq. (5) performed. It was found that 64-point Gaussian quadrature and 30-point Laguerre quadrature gave values for the integrals converged to at least six decimal places.

APPENDIX B: MORSE MATRIX ELEMENTS FOR r AND r^2

The Morse matrix elements in Ref. 21 for $r \equiv (R - R_0)$ were simplified to give

$$\langle v+j|r|v\rangle = \frac{(-1)^{j+1}}{a}\frac{[(k-2v-1)(k-2v-2j-1)]^{1/2}}{j(k-2v-j-1)} \times\left[\frac{(v+j)(v+j-1)\ldots(v+1)}{(k-v-1)(k-v-2)\ldots(k-v-j)}\right]^{1/2} \tag{B1}$$

and

$$\langle v|r|v\rangle = \frac{1}{a}\left[\ln k - \left(\sum_{m=1}^{p-1}\frac{1}{(p-m)+z} + \Phi(1+z)\right)\right.$$

$$+\sum_{j=1}^{v}\frac{1}{(k-v-j)}(1-\delta_{v0})\Bigg], \tag{B2}$$

where $\Phi(x)$ is the digamma function,[32] k denotes $\omega/\omega\chi$, and a denotes $(2\mu\omega\chi)^{1/2}/\hbar$. Also, μ is the reduced mass of the two particles having an internuclear separation R and

$$z = k - \mathrm{Int}(k), \quad p = \mathrm{Int}(k) - 1 - 2v, \tag{B3}$$

where $\mathrm{Int}(k)$ is the integer nearest to k from below.

The off-diagonal Morse matrix elements of r^2 are given by Gallas in Ref. 18(a). However, the diagonal matrix elements of r^2, when calculated from the formula given by Gallas,[18(a)] can in general pose serious numerical difficulties [see Ref. 18(b)]. They were instead calculated from the formula

$$\langle v|r^2|v\rangle \simeq \sum_{j\{\mathrm{bound}\}} \langle v|r|j\rangle\langle j|r|v\rangle, \tag{B4}$$

which assumes an approximate completeness relation

$$\sum_{j\{\mathrm{bound}\}} |j\rangle\langle j| \simeq 1 \tag{B5}$$

for the Morse oscillator bound states. For relatively low values of v, it is not expected that the contribution in Eq. (B4) from the continuum wave functions is significant.

APPENDIX C: TRANSFORMATION OF FORCE CONSTANTS FOR CHD_3 TO CHT_3

The transformation of the cubic and quartic force constants from CHD_3 normal mode coordinates to CHT_3 normal mode coordinates was performed in a straightforward way using the equations

$$\mathbf{q} = \mathbf{L}\mathbf{Q}, \quad \mathbf{q} = \mathbf{L}'\mathbf{Q}', \tag{C1}$$

where the primed quantities refer to CHT_3, the unprimed quantities refer to CHD_3, the $\mathbf{Q}$'s are the normal modes, and the $\mathbf{q}$'s are the internal symmetry coordinates (Table I). Equating the two expressions in Eq. (C1), one obtains

$$\mathbf{Q} = \mathbf{L}^{-1}\mathbf{L}'\mathbf{Q}', \tag{C2}$$

i.e.,

$$\mathbf{Q} = \mathbf{A}\mathbf{Q}', \tag{C3}$$

where

$$\mathbf{A} = \mathbf{L}^{-1}\mathbf{L}'. \tag{C4}$$

The cubic and quartic force constants for CHT_3 are then easily found to be

$$F'_{nlm} = \sum_{ijk} F_{ijk} A_{in} A_{jl} A_{km} \tag{C5}$$

and

$$F'_{nlmp} = \sum_{hijk} F_{hijk} A_{hn} A_{il} A_{jm} A_{kp}. \tag{C6}$$

In this case, A_{11} is defined to be equal to unity and the other A_{1i} and A_{i1} are set equal to zero. This was done because coordinate 1 is taken to be the local mode C–H stretching coordinate, and the normal mode transformation is performed independently of this coordinate.

APPENDIX D: MATRIX ELEMENTS OF $\tilde{G}$ FOR CH_3D

Let $\tilde{G}_{ij}(r_1,r_2,r_3)$ be any general normal mode transformed G-matrix element from Eq. (4.6c). The matrix elements [Eq. (4.8)] between CH_3 local mode states j and j' from manifolds with total C–H stretching quanta v and v' [the Γ indices from Eq. (4.8) have been suppressed] are

$$\langle v'j'|\tilde{G}_{ij}|vj\rangle = \sum_{i'=0}^{N'_0}\sum_{i=1}^{N_0} C^{j',v'}_{i',v'} {}^{*}\mathbf{G}_{i',i} C^{j,v}_{i,v}, \tag{D1}$$

where N_0 is the number of symmetrized zeroth order wave functions for the manifold with v C–H stretching quanta and

$$C^{j,v}_{i,v} = \langle v,i_0|v,j\rangle, \tag{D2}$$

with $|v,i_0\rangle$ being the symmetrized zeroth order wave function:

$$|v,i_0\rangle = \sum_{p}^{N_p} C^{i,v}_{p,v}|p;v\rangle. \tag{D3}$$

In Eq. (D3),

$$C^{i,v}_{p,v} = \langle p;v|v,i_0\rangle \equiv \text{the symmetrization coefficients,}[25] \tag{D4}$$

and N_p is the number of different permutations p of the unsymmetrized local mode state $|p;v\rangle$ with v total C–H quanta [in an abbreviated notation for Eq. (4.1)]. Furthermore,

$$\mathbf{G}_{i',i} = \sum_{p=1}^{N_p}\sum_{p'=1}^{N'_p} C^{i',v'}_{p',v'} {}^{*}\langle p';v'|\tilde{G}_{ij}|p;v\rangle C^{i,v}_{p,v}. \tag{D5}$$

The matrix elements $\langle p';v'|\tilde{G}_{ij}|p;v\rangle$ were computed numerically by the following procedure: (1) the standard G matrix in internal valence coordinates is calculated in terms of the atomic masses and the quantities $\langle v_i|r_i^{-1}|v'_i\rangle\delta_{v_jv'_j}\delta_{v_kv'_k}$, $\langle v_i|r_i^{-2}|v'_i\rangle\delta_{v_jv'_j}\delta_{v_kv'_k}$, and $\langle v_iv_j|(r_i\,r_j)^{-1}|v'_iv'_j\rangle\delta_{v_kv'_k}$, where $|v_i\rangle$, $|v'_i\rangle$, etc. are Morse oscillator eigenfunctions[17,18] appropriate to the states $|p;v\rangle$ and $|p';v'\rangle$; (2) the symmetry coordinate transformation [Eq. (3.5)] is performed with the symmetry coordinates from Table VII; (3) the normal mode transformation [Eq. (3.4)] is performed with the $\mathbf{L}^{-1}$ matrix calculated from the normal mode analysis of Eq. (4.5). As before, the three C–H coordinates were excluded from this transformation. The ijth term of this matrix of values corresponds to the matrix element $\langle p';v'|\tilde{G}_{ij}|p;v\rangle$. This procedure yields values for the matrix elements in Eq. (D1) efficiently and economically. A direct multidimensional numerical integration in terms of the three C–H coordinates was anticipated to be too expensive and, because of the dependence on several coordinates, probably inaccurate.

APPENDIX E: CORIOLIS INTERACTION AND LOCAL MODE DEGENERACY

In order to determine whether Coriolis interactions can strongly effect the threefold near degeneracy of the zeroth order states in Eqs. (4.9)–(4.10c) for the present model of CH_3D, a simple calculation was performed to estimate these effects for the pure A_1, E_a, and E_b symmetrized zeroth order CH_3 local mode states[25]

$$|\psi_1;A_1\rangle = \frac{1}{\sqrt{3}}(|v,0,0\rangle + |0,v,0\rangle + |0,0,v\rangle), \quad \text{(E1)}$$

$$|\psi_2;E_a\rangle = \frac{1}{\sqrt{6}}(2|v,0,0\rangle - |0,v,0\rangle - |0,0,v\rangle), \quad \text{(E2)}$$

and

$$|\psi_3;E_b\rangle = \frac{1}{\sqrt{2}}(|0,v,0\rangle - |0,0,v\rangle). \quad \text{(E3)}$$

In this calculation, a rectilinear coordinate treatment was used due to the relative simplicity of the equations in this approach.[33] In addition, it is well known that the description of molecular vibrations in the curvilinear coordinate approach differs most strongly from the rectilinear treatment only for the bending modes.[5,6] For these reasons and because we only desire to estimate these rotational effects, the rectilinear coordinate approach is well suited to our purpose.

The first order Coriolis effect is described in the small amplitude limit by the vibration/rotation coupling term[33]

$$V_{vr} = -\frac{\hat{P}_z \hat{p}_z}{I_z}, \quad \text{(E4)}$$

where $\hat{P}_z$ is the z projection of the rotational angular momentum, $\hat{p}_z$ is the z projection of the vibrational angular momentum, and I_z is the z component of the inertia tensor (taken as a constant). The orientation of the molecule is such that the z axis in the body fixed coordinate system is along the symmetry axis of the molecule. The contribution to this term from the CH_3 local mode coordinates r_1, r_2, and r_3 is

$$V'_{vr} = -\frac{\hat{P}_z}{I_z}\sum_{i<j}^{3}\zeta^z_{ij}(\hat{r}_i\hat{p}_j - \hat{r}_j\hat{p}_i), \quad \text{(E5)}$$

where the ζ^z_{ij} are the Coriolis zeta constants,[33,34] and $\hat{p}_i$ is the momentum operator conjugate to $\hat{r}_i$. The first order matrix elements are then (with $\hbar = 1$)

$$E^{(1)} = -\frac{K}{I_z}\langle\psi_i;\Gamma|C(\hat{\mathbf{r}},\hat{\mathbf{p}})|\psi_{i'};\Gamma'\rangle, \quad \text{(E6)}$$

where $C(\hat{\mathbf{r}},\hat{\mathbf{p}})$ is the summation term in Eq. (E5) and the states $|\psi_i;\Gamma\rangle$ are states from Eqs. (E1)–(E3). The zeta constants for the coordinate system defined by the normal mode transformation of Eq. (4.5) (excluding the C–H coordinates) and the three C–H stretching coordinates were calculated using standard techniques.[34] The values for these constants were found to be $\zeta^z_{12} = -\zeta^z_{13} = \zeta^z_{23} = 0.06$. The values of the x and y zeta constants ζ^x_{ij} and ζ^y_{ij} were also calculated and found to be even smaller. As a check of the present method, a complete normal mode calculation was performed (including the C–H coordinates), and we reproduced exactly all of the relevant normal mode zeta constants for CH_3D (see Table VI of Ref. 20).

In standard normal mode theory,[33] the matrix element [Eq. (E6)] between doubly degenerate normal modes of E symmetry yields the value $-(K/I_z)(\pm l_i)\delta_{ii'}\delta_{\Gamma\Gamma'}$, where l_i is the magnitude of the vibrational angular momentum of degenerate state i, and hence splits the degeneracy of this mode due to the difference in the values of the diagonal elements. For the local mode states [Eqs. (E1)–(E3)], the matrix element in Eq. (E6) was evaluated numerically. It was found that the only nonzero first order matrix element is between the E_a state [Eq. (E2)] and the E_b state [Eq. (E3)] and, for $v = 6$, that it is extremely small ($\sim 4\times10^{-7}$ cm^{-1}).

The second order Coriolis interactions of the states in Eqs. (E1)–(E3) with the symmetrized zeroth order local mode combination states of $|5,1,0\rangle$ parentage were next calculated. To do this, a Van Vleck transformation[35] through second order was employed in order to treat the problem by a simple 2×2 matrix for the states (E2) and (E3) with $v = 6$. The only nonzero perturbations were the first order corrections just described and diagonal second order corrections arising from the coupling to the E symmetry combination states of $|5,1,0\rangle$ parentage. These interactions were again found to be very small ($\sim 10^{-2}$ cm^{-1}). It is clear that, while the degeneracy of the local mode states (E1)–(E3) is lifted by the Coriolis interactions, this effect is expected to be entirely negligible on the scale of Fig. 4 and thus contributes little to the observed spectral congestion. The weakness of these interactions is primarily due to the smallness of the zeta constants ζ^z_{ij} for the local mode coordinates appearing in Eq. (E5) and because the local mode states presumably have very little vibrational angular momentum. Whether Coriolis effects are important for the pure local mode states in other molecules with different symmetries remains an open question.[36] It is also again emphasized that the above calculations assume the local axial symmetry of the CH_3 group in the CH_3D molecule.

[1]For reviews, see (a) B. R. Henry, Acc. Chem. Res. **10**, 207 (1977); (b) H. L. Fang and D. L. Swofford, *Advances in Laser Chemistry*, edited by B. A. Garetz and J. R. Lombardi (Heyden, London, 1982); (c) M. L. Sage and J. Jortner, Adv. Chem. Phys. **47**, 293 (1981).

[2]J. W. Perry, D. J. Moll, A. Kuppermann, and A. H. Zewail, J. Chem. Phys. (in press).

[3]See, for example, W. Kaye, Spectrochim. Acta **6**, 257 (1954); H. L. Fang and R. L. Swofford, J. Chem. Phys. **72**, 6382 (1980); O. Sonnich Mortensen, B. R. Henry, and M. A. Mohammadi, *ibid.* **75**, 4800 (1981).

[4](a) E. L. Sibert III, W. P. Reinhardt, and J. T. Hynes, Chem. Phys. Lett. **92**, 455 (1982); (b) E. L. Sibert III, Ph.D thesis, University of Colorado, Boulder, 1983; (c) E. L. Sibert III, W. P. Reinhardt, and J. T. Hynes, J. Chem. Phys. **81**, 1115 (1984); E. L. Sibert III, J. T. Hynes, and W. P. Reinhardt, *ibid.* **81**, 1135 (1984).

[5]R. Meyer and H. H. Günthard, J. Chem. Phys. **49**, 1510 (1968); L. A. Gribov, Opt. Spectrosc. **31**, 842 (1971); H. M. Pickett, J. Chem. Phys. **56**, 1715 (1972); C. R. Quade, *ibid.* **64**, 2783 (1976); **79**, 4089 (1983); W. B. Clodius and C. R. Quade, *ibid.* **80**, 3528 (1984).

[6]A. R. Hoy, I. M. Mills, and G. Strey, Mol. Phys. **24**, 1265 (1972).

[7]E. L. Sibert III, J. T. Hynes, and W. P. Reinhardt, J. Phys. Chem. **87**, 2032 (1983).

[8]E. B. Wilson Jr., J. C. Decius, and P. C. Cross, *Molecular Vibrations* (McGraw–Hill, New York, 1955), p. 74.

[9]M. L. Sage and J. Jortner, Chem. Phys. Lett. **62**, 451 (1979); P. R. Stannard and W. M. Gelbart, J. Phys. Chem. **85**, 3592 (1981).

[10]J. W. Perry and A. H. Zewail, J. Phys. Chem. **85**, 933 (1981).

[11]W. P. Reinhardt (private communication to A. H. Zewail regarding theoretical predictions of these differences in linewidth).

[12]For reviews, see D. W. Noid, M. L. Koszykowski, and R. A. Marcus, Annu. Rev. Phys. Chem. **32**, 267 (1981); S. A. Rice, Adv. Chem. Phys. **47**, 117 (1981).

[13]A. H. Zewail, Physics Today **30**, No. 11 (1980).

[14]Reference 8, p. 364.

[15]S. M. Lederman (private communication).

[16]Reference 8, Chap. 4.

[17]P. M. Morse, Phys. Rev. **34**, 57 (1929).

[18](a) J. A. C. Gallas, Phys. Rev. A **21**, 1829 (1980); (b) V. S. Vasan and R. J. Cross, J. Chem. Phys. **78**, 3869 (1983).
[19]S. Califano, *Vibrational States* (Wiley, New York, 1976), Chap. 9.
[20](a) D. L. Gray and A. G. Robiette, Mol. Phys. **37**, 1901 (1979); (b) The value of F_{56} in Eq. (3.18) was calculated from the Gray and Robiette surface, and we made no effort to find an improved value so as to better fit the data at $v = 7$; (c) The quadratic force constants from Ref. 20(a) are assumed to be reasonably accurate. The potential parameters in their work are derived primarily from experimental and *ab initio* studies for low excitation in the C–H and other modes.
[21]L. Halonen and M. S. Child, Mol. Phys. **46**, 239 (1982).
[22]J. Mathews and R. L. Walker, *Mathematical Methods of Physics* (Benjamin, Menlo Park, California, 1970), pp. 387–393.
[23]M. L. Sage, J. Phys. Chem. **83**, 1455 (1979).
[24]O. S. Mortensen, B. R. Henry, and M. A. Mohammadi, J. Chem. Phys. **75**, 4800 (1981).
[25]L. Halonen and M. S. Child, J. Chem. Phys. **79**, 4355 (1983).
[26]See, for instance, K. E. Jones, A. H. Zewail, and D. J. Diestler, in *Advances in Laser Chemistry*, edited by A. H. Zewail (Springer, Berlin, 1978), p. 258.
[27]S. M. Lederman and R. A. Marcus, J. Chem. Phys. **81**, 5601 (1984).
[28]H. R. Dübal, M. Lewerenz, and M. Quack, Faraday Discuss. Chem. Soc. **75**, 358 (1983); K. von Puttkamer, H. R. Dübal, and M. Quack, *ibid.* **75**, 197 (1983).
[29]S. Peyerimhoff, M. Lewerenz, and M. Quack, Chem. Phys. Lett. **109**, 563 (1984).
[30]P. M. Felker and A. H. Zewail, Chem. Phys. Lett. **102**, 113 (1983); Phys. Rev. Lett. **53**, 501 (1984).
[31]*Handbook of Mathematical Functions*, edited by M. Abramowitz and I. A. Stegun (Dover, New York, 1965), Chap. 25.
[32]Reference 31, Chap. 6.
[33]J. E. Wollrab, *Rotational Spectra and Molecular Structure* (Academic, New York, 1967), Chap. 3.
[34]Reference 19, p. 97.
[35]Reference 33, Appendix 7.
[36]I. Abram, A. de Martino, and R. Frey, J. Chem. Phys. **76**, 5727 (1982).